Eur Biophys J (2001) 30: 63–68
DOI 10.1007/s002490100136

ARTICLE

Francesca Natali · Frank Schmithüsen

Co-rebinding in myoglobin as seen by time-resolved X-ray absorption spectroscopy

Received: 17 July 2000 / Revised version: 4 January 2001 / Accepted: 4 January 2001 / Published online: 6 March 2001

Abstract The dynamics of selected conformational coordinates, key roles in the understanding of the CO-rebinding process, are investigated in horse heart carbonmonoxy myoglobin (MbCO) through time-resolved X-ray absorption spectroscopy. We present here the results obtained at 90 K in the second time scale. The approach of the CO molecule towards the Fe atom in the active site pocket is speculated to act as a natural precursor to the Fe displacement with the consequent undoming of the protein porphyrin plane. The arrangement of the Fe-C-O bonding angle geometry follows and the final MbCO active site configuration is completely reached within 1 min.

Key words Myoglobin · Carbon monoxide recombination · Protein dynamics · Time-Resolved X-ray Absorption Spectroscopy · Turbo X-ray Absorption Spectroscopy

Introduction

Despite the large number of efforts made to understand the structure-function relationship in proteins, no uncontroversial description is available. Major investigations have been carried out on myoglobin, considered as a model, for simplicity. Indeed, myoglobin (Mb) is a small protein that stores and transports dioxygen in muscles. The folded polypeptide chain of Mb embeds a heme group with a central iron atom, bonded with small ligands. In carbonmonoxy myoglobin (MbCO) a CO molecule is bound to the heme iron and the covalent bond between the iron and the CO is broken upon absorption of visible light (e.g. laser flash or extended illumination).

MbCO and Mb possess different structures and ligand dissociation initiates a conformational relaxation from a structure still close to the bound state towards the deoxy-like structure (Mb*). Below about 180 K, the rebinding after photodissociation is non-exponential in time. Austin et al. (1975) explained this behaviour as due to static distribution of protein conformations. At low temperature (< 180 K) the ligand cannot exit the protein and the binding occurs directly from the heme pocket (Ansari et al. 1987; Lim et al. 1995; Ostermann et al. 2000). Moreover, each protein molecule is frozen in its local conformational minimum and no fluctuations between substates are observed (Elber and Karplus 1987).

The existence of a protein conformational landscape is confirmed by a growing set of experimental data (Doster et al. 1989; Frauenfelder et al. 1988; Hong et al. 1990; Parak et al. 1987). In particular, experiments such as optical, Fourier Transform Infrared (FTIR) and X-ray Absorption (XAS) Spectroscopies have shown that the conformational landscape of the different equilibrium forms of the protein (e.g. the bound MbCO and unbound Mb) and the structural intermediates in the ligand binding process are strictly affected by the environmental conditions such as pH, temperature, sugar matrices, etc. (Bianconi et al. 1999; Cordone et al. 1998; Gottfried et al. 1996; Hagen et al 1995, 1996; Natali et al. 1998).

The iron site structure of Mb and MbCO determined by both X-Ray Diffraction (XRD) and Extended X-ray Absorption Fine Structure (EXAFS) is characterized by an average Fe-N_p distance (where N_p stands for heme pyrrolic nitrogen) of 2.06 Å in Mb and 2.01 Å in MbCO (Bianconi et al. 1988; Chance et al. 1983; Fermi et al. 1981; Kuriyan et al. 1986; Phillips 1981; Powers et al. 1984, 1987; Takano 1977).

The protein relaxation after photolysis is reported to be related to changes in the stereochemistry of the heme

F. Natali (✉)
INFM, Operative Group in Grenoble CRG-IN13,
ILL, 6 Avenue J. Horowitz, BP 156,
38042 Grenoble Cedex 9, France
E-mail: natali@ill.fr
Tel.: +33-4-76207071
Fax: +33-4-76483906

F. Natali · F. Schmithüsen
European Synchrotron Radiation Facility, Grenoble, France

iron; it is found that the iron moves out of the plane towards the proximal ligand, followed by the N_p atoms. In particular, a distance Fe-$N_p = 2.03 \pm 0.02$ Å for Mb* in frozen solutions at 4–20 K has been reported (Powers et al. 1984). An additional structural change involves a translation of the F helix across the heme as the global protein structure relaxes in response to the conformational change of the heme. More recent results have been obtained by Chu et al. (2000) as well as by Lim et al. (1997) on the CO trajectory after photodissociation in myoglobin. In particular, ultrafast rotation and trapping of the CO molecule, in the approaching of a docking site close to the Fe atom, is suggested.

Here we report complementary and unique information on the modification of the active site structure by X-ray Absorption Near Edge Structure (XANES) spectroscopy (Bianconi et al. 1988; Della Longa et al. 1995; Zhang et al. 1989), which is a fast (10^{-15} s) and atomic selective structural tool to obtain information on heme local structure (Bianconi et al. 1985a; Pin et al. 1994). In fact, XANES provides the statistical average of the iron site conformations in heme proteins, spanned during protein fluctuations (Bianconi et al. 1985b). Moreover, the major limitation in the investigation of protein structure and dynamics through transmission XAS experiments has been overcome. Indeed, the performance of a dispersive optical geometry facility (Hagelstein et al. 1997) has been here extended, allowing us to perform time-resolved experiments by parallel data collection.

This technique, named "Turbo-XAS" (Pascarelli et al. 1999), taking advantage of the absence of optical elements movement, overcomes the spectrum aberration arising from inappropriate normalization procedures by simultaneously recording of I_0 and I_1 intensities. Indeed, this is one of the major problems occurring in transmission experiments with extremely diluted samples, being particularly sensitive to beam instability and sample inhomogeneity.

Our previous work (Bianconi et al. 1999) has shown how, by following the dynamics of selected features in the XANES spectra, important information can be obtained. Different kinetics for the CO-rebinding in horse-heart MbCO were found in such a way for two particular conformational coordinates: (1) the doming of the heme plane, described by the displacement of the Fe atom from a planar configuration with respect to the pyrrolic macrocycle, and (2) the Fe-C-O bonding angle geometry, covering the latter in a longer time scale. These results were obtained by using a novel experimental technique named "Temperature Derivative XAS" (TDXAS) (Berendzen and Brauenstein 1990; Filipponi 1996), consisting of following the absorption intensity at fixed energy values in the XANES spectrum while varying linearly the sample temperature, after previous Fe-CO photodissociation performed at 25 K by continuous sample illumination.

In this work we present results on the temporal evolution of the same conformational coordinates at a fixed temperature, namely 90 K, occurring during relaxation after Fe-CO photodissociation performed under the same experimental conditions. In particular, we report here on the direct evidence of at least two intermediate states reached by the protein during the CO rebinding, each of them being characterized by a different overall structural configuration.

Material and methods

Lyophilized horse-heart Mb was purchased from Sigma (St. Louis, Mo., USA). Mb met solution was obtained by dissolving an appropriate amount of dried ferric protein in 0.2 M phosphate buffer ($Na_2HPO_4 + NaH_2PO_4$ H_2O, pH 7, at room temperature) in water to give a suitable protein concentration for X-ray absorption measurements (~10 mM). The solution was centrifuged, equilibrated with CO and reduced by anaerobic addition of sodium dithionite to reach the MbCO state.

The sample was cooled down using a nitrogen cryojet and the temperature was monitored with a PID controller with an accuracy of ±1 K. A nitrogen gas flux prevented the sample from undesired air condensation on the windows of the sample holder, which would lead to aberration in the absorption spectra.

Photodissociation was performed by continuously illuminating the sample for about 90 min, by means of two high-power fibre optic lamps. The sample was irradiated from both faces in order to ascertain homogeneous and complete photodissociation.

The Fe-CO recombination process was monitored at 90 K, the lowest temperature reachable with the cryojet. Indeed, no standard helium closed-cycle cryostat was suitable for transmission measurement of diluted samples owing to inevitable compressor vibration, which was shown to affect the data quality. At this temperature value, the percentage of non-rebounded molecules has been reported in the literature (Frauenfelder et al. 1991) to be ~20% at 1 s after the photodissociation occurs and less than 3% after 90 s. As explained in detail in the Results and discussion section, the Turbo-XAS technique has allowed us to cover this time scale to explore the CO-rebinding kinetics.

The X-ray absorption spectra of MbCO were measured at the ESRF synchrotron radiation facility in Grenoble on the ID24 beamline. The 6 GeV storage ring was operating in 2/3 fill mode with a typical current of 180 mA.

ID24 is the ESRF dispersive XAS beamline, with parallel detection of the whole spectrum made possible by energy dispersive highly focusing X-ray optics. The focal spot size on the sample position was measured to be 200 × 200 μm ($H \times V$ FWHM), small enough to measure inside the cryojet target, and large enough (1) to prevent the sample from radiation damaging, already reduced by the low temperature working condition (90 K) and (2) to average on a bigger sample portion, i.e. reducing sample inhomogeneity effects.

In this experiment the performances of the beamline were extended by scanning the incoming beam with narrow slits (~50 μm aperture) placed just after the elliptically curved polychromator, as described in detail elsewhere (Pascarelli et al. 1999). Data were collected simultaneously with the slit movement. The energy resolution was obviously strictly related to the slit aperture (Pascarelli et al. 1999). Moreover, the number of total points acquired was dependent strongly on the energy range explored and on the speed of the scanning slit motor, the acquisition time for each point being fixed to 400 μs. The upper motor speed limit was mainly governed by the onset of oscillating behaviour in the slit motion, resulting in the degradation of the energy resolution.

The data here reported cover a spanned energy range of about 160 eV at the Fe K-edge with 3000 points (binned to give 250 final points). The intensities of the incoming and outcoming beams were measured by means of two ionization chambers, placed before and after the sample position respectively, and successively amplified by a fast current amplifier.

A total number of 360 spectra was collected, the first 10 spectra corresponding to the system in the photodissociated state (Mb*) induced under light illumination, while the following 350, covering 5 min of total acquisition time, were acquired during the sample relaxation towards the MbCO state.

Results and discussion

The measured X-ray absorption coefficient $\mu(E)$ for electronic transtions from the core Fe 1s level to unoccupied final states is given by the product of the matrix element times the joint density of states, according with the Fermi golden rule. It has been shown that it can be solved in real space (Bianconi et al. 1988; Zhang et al. 1989) and can be written as:

$$\mu(E) = \mu_0(E)\left[1 + \sum\nolimits_{n\geq 2} \chi_n(E)\right] \quad (1)$$

where $\mu_0(E)$ is the so-called atomic absorption coefficient for the selected 1s level of the isolated Fe ion with its Muffin Tin potential. The modulation factor:

$$\chi(E) = \sum\nolimits_{n\geq 2} \chi_n(E) = [\mu(E) - \mu_0(E)]/\mu_0(E) \quad (2)$$

is due to a type of electron diffraction where the Fe ion plays both the role of source and detector. Therefore it probes the positions of the neighbour atoms as seen from the Fe atom. In fact, $\chi_n(E)$ is the contribution arising from all multiple scattering pathways of the excited photoelectron beginning and ending at the central absorbing atom and involving (n–1) neighbour atoms (Bianconi et al. 1985a, 1988; Della Longa et al. 1995; Pin et al. 1994; Zhang et al. 1989).

In Fig. 1 the Fe K-edge spectrum of a standard Fe metal foil, measured by the Turbo-XAS technique, is shown. The pre-edge background was subtracted and the absorption coefficient has been normalized to the atomic absorption jump for transition from the Fe 1s level to the continuum.

The XANES of the Fe foil allows the energy calibration, i.e. the correlation between the slit absolute position and the spanning energy. A total energy range of about 160 eV was obtained by spanning the slits in less than 1.2 s. On the other hand, the enhancement of the characteristic features of the metal Fe spectrum (Fig. 1) ascertains the choice of slit aperture (50 μm) in respect of the energy resolution.

The magnified XANES region of the MbCO absorption spectrum, measured at $T = 90$ K, is shown in Fig. 2, corresponding to the average over the first 10 consecutive spectra (with ~18 s of total acquisition time), i.e. to the protein in the photodissociated state (Mb*). The zero of the energy scale (E_0) has been fixed at the Fe metal K-edge defined as the first maximum of its derivative spectrum: $E_0 = 7111.2$ eV.

Even though we were not able to resolve the characteristic features of the pre-edge region (this would require much higher energy resolution), the comparison with previously acquired fluorescence spectra has shown extremely good agreement.

In order to reduce the dead time between two spectra acquisitions down to the intrinsic motor hardware limit ($t_i = 0.25$ s corresponds to the acceleration and deceleration of the motor), the acquisition was made keeping its movement in both directions. Minor adjustments were compensating for the eventual fictive energy shifts of the edge position, arising from motor backlash corrections. With this procedure, each selected energy value (E_j) was successively explored with the following time delay:

$$t_{2n-1}(E_J) = (n-1) \times 2t_{\text{tot}} + (t_i + t_0(E_J)) \quad (3)$$

$$t_{2n}(E_J) = n \times 2t_{\text{tot}} - (t_i + t_0(E_J)) \quad (4)$$

where n ($n = 0, 1, 2,...$) represent the cycle number ($2n$ and $2n$–1 referring to the particular movement direction), $t_0(E_j)$ the time needed to reach the E_j energy position for the first time ($0 < t_0 < 1.2$ s), and $t_{\text{tot}} = 2t_i + 1.2$ s.

In Fig. 3 we show the spectrum difference $A_{\text{Mb*}} - A_{\text{MbCO}}$, where the $A_{\text{Mb*}}$ (dashed curve) and A_{MbCO} (dotted curve) correspond to the absorption intensities

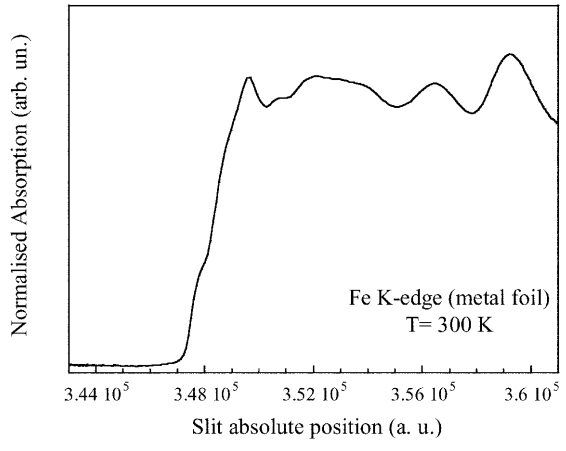

Fig. 1 Normalized Fe K-edge XANES spectrum of standard Fe metal foil measured using the Turbo-XAS technique

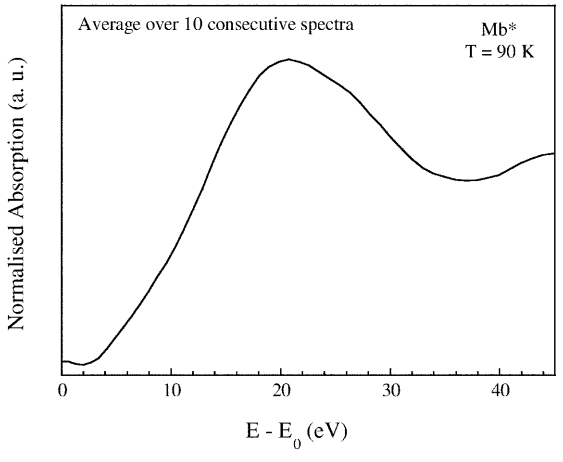

Fig. 2 Normalized Fe K-edge MbCO XANES spectrum, averaged over 10 consecutive spectra, measured at $T = 90$ K

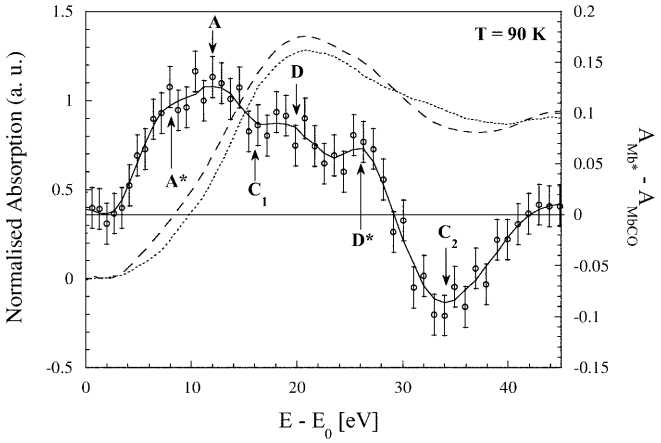

Fig. 3 *Solid line*: Fe K-edge Mb*-MbCO absorption spectrum difference, measured at 90 K. The spectra of Mb* (*dashed curve*) and MbCO (*dotted curve*) are also shown

averaged over the first 10 spectra (1–10) and last 10 spectra (350–360), measured at 90 K after and before sample illumination, respectively. The error bars ($\pm 4 \times 10^{-2}$) have been calculated from the error propagation formula, the uncertainty of the absorption intensity in a single XANES spectrum being 3×10^{-2}.

As described in detail elsewhere (Bianconi et al. 1985a, 1985b, 1988; Della Longa et al. 1995; Pin et al. 1994; Zhang et al. 1989), the main features displayed in Fig. 3 are closely related to the structural parameter of the iron active site. In particular, the A* and A peaks, placed at 8 and 12 eV from the edge respectively, arise from the planar scattering of the photoelectron pathway and provide information on (1) the distance between the iron atom and the pyrrolic nitrogens, (2) the net charge around the Fe atom and (3) the coordination number. The intensity of feature A ($\sim 1.5 \times 10^{-1}$) confirms here that the photodissociation process was complete.

Changes in the intensities of the D (20 eV) and D* (26 eV) peaks, due as well to planar scattering, were shown to reflect doming effects, i.e. distortion of the heme plane, the intensity of the D peak increasing with the distortion of the tetrapyrrolic macrocycle (Cartier et al. 1992). A structural mechanism related to this spectral transition includes a Fe atom slightly closer to the average plane of the pyrrolic nitrogens in the lower state and/or distortion of the heme plane (enhancing the intensity of D).

On the other hand, the C_1 (16 eV) and C_2 (34 eV) peaks, originating from the axial scattering, contain information on the active site geometry and in particular on the Fe-C-O bonding angle: a larger intensity of the C_1 and C_2 peaks reflects a more linear Fe-C-O configuration (Bianconi et al. 1985a; Cartier et al. 1992; Della Longa et al. 1994; Ormos et al. 1988).

We have chosen to follow selectively the temporal evolution of the D and C_2 peaks, placed at 20 eV and 34 eV after the Fe K-edge, respectively. This was to analyse separately the doming of the heme plane and the Fe-C-O bonding angle geometry in the process of reaching the final configuration.

In Fig. 4 the temporal behaviour of the $A(t)$–$A(0)$ absorption intensity difference of the above-mentioned D and C_2 peaks (panels a and b, respectively) are shown. In order to gain in statistics, necessary to reveal extremely small absorption intensity variations, each point is taken as the average over five points, centred on the peak position, and over two spectra, giving rise to a final uncertainty of 2×10^{-2}. As expected, the CO-rebinding process investigated at 90 K covers a time range of ≤ 90 s, within the experimental uncertainty.

As already described, the intensity variation of the two features (D and C_2) arises mainly from a modification of the planar and axial scattering of the photoelectron pathway, respectively. However, the data quality, owing to the low Fe atom concentration, is still insufficient to perform quantitative investigation by fitting the experimental data with theoretical curves obtained with multiple scattering calculations. The time dependence of the D and C_2 absorption intensities are divided into four different regions, which we propose to be related to the existence of at least four different states explored by the protein during the CO-recombination process, characterized by an overall different structural

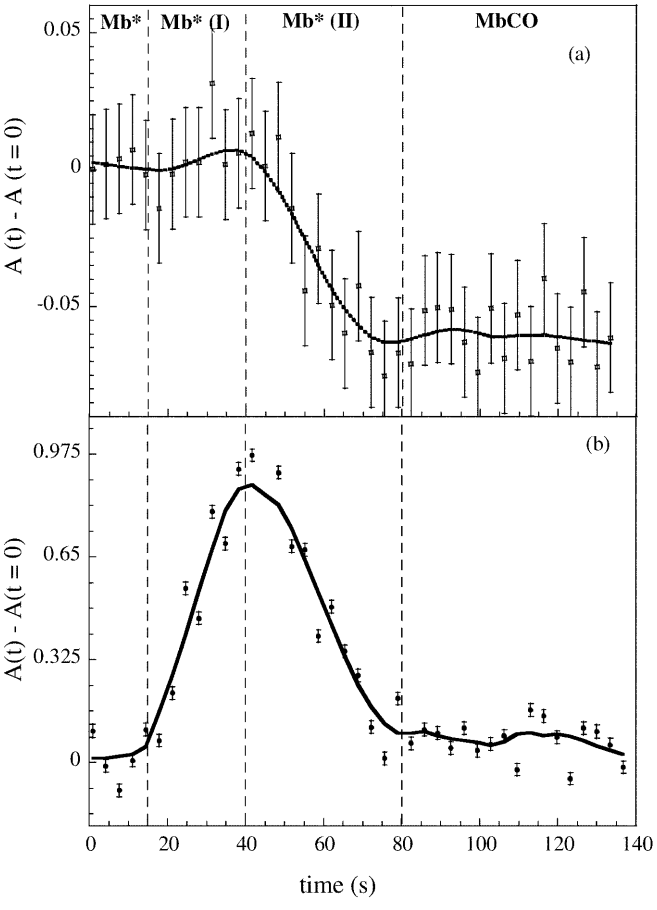

Fig. 4 Temporal behaviour of the $A(t)$–$A(0)$ absorption intensity differences of the D and C_2 peaks (**a** and **b**, respectively)

configuration involving the doming of the heme plane and Fe-C-O bonding angle geometry.

State Mb*

Until the protein molecule is perturbed by continuous illumination ($0 < t < 20$ s) the system is in equilibrium in a first state (Mb*) with a modest displacement of the CO molecule with respect to the Fe atom; the sample temperature is indeed too low (90 K) to promote the migration of the CO molecule from the heme pocket to the solvent (Lim et al. 1995; Ostermann et al. 2000). The porphyrin plane is domed with the Fe atom out of the porphyrin plane and closer to the proximal histidine.

State Mb*(I)

As soon as the illumination of the sample is ended ($20 < t < 40$ s), the relaxation process begins. A first intermediate state, namely phase Mb*(I), takes place, characterized by the approach of the CO molecule towards the heme plane (i.e. towards the iron atom) and resulting in an increasing of the axial scattering intensity due mainly to van der Waals interactions. This could support the idea of a rotation of the CO molecule around the Fe atom, as suggested by Chu et al. (2000) and Lim et al. (1997). On the other hand, the stationary intensity of the planar scattering (peak D) suggests that the heme plane configuration is not affected.

State Mb*(II)

At $t = 40$ s (i.e. 20 s after ending the sample illumination) the intensity of the C_2 feature reaches its maximum value and we support the idea that the CO molecule bonds covalently to the iron atom in a configuration perpendicular with respect to the heme plane (maximal axial scattering). A second intermediate state [phase Mb*(II)] now takes place ($40 < t < 80$ s) and a decreasing of both the axial and planar scattering intensities is observed. This suggests that, simultaneously with the approaching of the iron atom towards the in-plane configuration, with consequent undoming of the phorphyrin plane, the Fe-C-O starts to softly bend (Bianconi et al. 1985a; Lim et al. 1995; Ostermann et al. 2000), reflecting the decreasing axial scattering intensity to reach its final configuration (MbCO phase).

State MbCO

At $t = 80$ s an almost axial Fe-C-O bonding angle geometry and a complete planar configuration of the heme plane with the iron atom placed on its centre is reached. The final equilibrium is proved by the stationary behaviour of both intensities over a long time range.

Conclusions

The Turbo-XAS technique has been here proved to be an optimal tool for time-resolved X-ray transmission investigation of protein dynamics, overcoming the known limitation of biological compounds owing to the low absorbing atoms concentration.

The results suggest the existence of at least two intermediates states [Mb*(I) and Mb*(II)] reached by the protein during the CO-rebinding process. These phases are shown to be characterized by a different overall structural configuration of the Fe active site. In particular, it has been observed that the undoming of the porphyrin plane and the Fe-CO bonding angle relaxation occur with different CO-rebinding rates.

Acknowledgements We thank the ID24 beamline staff for their help and cooperation during the experimental run.

References

Ansari A, Berendzen J, Cowen BR, Fraunefelder H, Hong MK, Iben IET, Johnson JB, Ormos P, Sauke TB, Scholl R, Schulte A, Steinbach PJ, Vittitow J, Young RD (1987) Rebinding and relaxation in the myoglobin pocket. Biophys Chem 26:337–355

Austin RH, Benson KW, Einstein L, Frauenfelder H, Gunsalus IC (1975) Dynamics of ligand binding to myoglobin. Biochemistry 14:5355–5373

Berendzen J, Brauenstein D (1990) Temperature derivative spectroscopy: a tool for protein dynamics. Proc Natl Acad Sci USA 87:1–5

Bianconi A, Congiu Castellano A, Durham PJ, Hasnain SS, Phillips S (1985a) The CO bond angle of carboxymyoglobin determined by angular-resolved XANES spectroscopy Nature 318:685–687

Bianconi A, Congiu Castellano A, Dell'Ariccia M, Giovannelli A, Burattini E, Durham PJ (1985b) Increase of the effective charge in hemoproteins during oxygenation process. Biochem Biophys Res Commun 131:98–102

Bianconi A, Garcia J, Benfatto M (1988) XANES in condensed systems. Top Curr Chem 145:29–67

Bianconi A, Natali F, Alosi ML, Grande S, Lanzara A, Saini NL, Brunelli M (1999) TDXAS study of the conformational landscape of MbCO. J Synchr Radiat 6:389–391

Cartier C, Momentau M, Dartyge E, Fontaine A, Tourillon G, Bianconi A, Verdaguer M (1992) X-ray absorption spectroscopy of carbonyl basket-handle Fe(II) porphyrins: distortion of the tetrapyrrolic macrocycle. Biochim Biophys Acta 1119:169–174

Chance B, Fischetti R, Powers L (1983) Structure and kinetics of the photoproduct of MbCO at low temperature: an X-ray absorption study. Biochemistry 22:3820–3829

Chu K, Vojtchovsky J, McMahon BH, Sweet RM, Berendzen J, Schlichting I (2000) Structure of a ligand-binding intermediate in wild-type carbonmonoxy myoglobin. Nature 403:921–923

Cordone L, Galajda P, Vitrano E, Gassmann A, Ostermann A, Parak F (1998) A reduction of protein specific motions in CO-ligated myoglobin embedded in a trehalose glass. Eur Biophys J 27:173–176

Della Longa S, Ascone I, Congiu Castellano A, Bianconi A (1994) Intermediates states in ligand photodissociation of carboxymyoglobin studied by dispersive x-ray absorption. Eur Biophys J 23:361–368

Della Longa S, Soldatov A, Pompa M, Bianconi A (1995) Atomic and electronic structure probed by X-ray absorption

spectroscopy: full multiple scattering analysis with G4XANES package. Comput Mater Sci 4:199–210
Doster W, Kusack S, Petry W (1989) Dynamic transition of myoglobin revealed by inelastic neutron scattering. Nature 337:754–756
Elber R, Karplus M (1987) Multiple conformational states of proteins: a molecular dynamics analysis of myoglobin. Science 235:318–321
Fermi G, Perutz MF, Shaanan B, Fourme R (1981) The crystal structure of human deoxyhaemoglobin at 1.74 Å resolution. J Mol Biol 175:159–174
Filipponi A (1996) Short-range order in liquid matter probed by high temperature X-ray absorption measurements. J Phys Condens Matter 8:9335–9339
Frauenfelder H, Parak F, Young RD (1988) Conformational substates in proteins. Annu Rev Biophys Chem 17:451–479
Frauenfelder H, Sligar SG, Wolynes PG (1991) The energy landscapes and motions of proteins. Science 254:1598–1603
Gottfried DS, Peterson ES, Sheikh AG, Wang J, Yang M, Friedman JM (1996) Evidence for damped hemoglobin dynamics in a room temperature trehalose glass. J Phys Chem 100:12034–12042
Hagelstein M, San Miguel A, Ressler T, Fontaine A, Goulon J (1997) The beamline ID24 at the ESRF for energy dispersive X-ray absorption spectroscopy. J Phys IV 1:302–303
Hagen SJ, Hofrichter J, Eaton WA (1995) Protein reaction kinetics in a room-temperature glass. Science 269:959–962
Hagen SJ, Hofrichter J, Eaton WA (1996) Germinate rebinding and conformational dynamics of myoglobin embedded in a glass at room temperature. J Phys Chem 100:12008–12021
Hong K, Brauenstein D, Cowen BR, Frauenfelder H, Iben IET, Mourant ER, Ormos P, Scholl R, Schulte A, Steinbach PJ, Xie H, Young RD (1990) Conformational substates and motions in myoglobin. Biophys J 58:429–436
Kuriyan J, Wilz S, Karplus M, Petsko GA (1986) X-ray structure and refinement of carbon monoxy (FeII)-myoglobin at 1.5 Å resolution. J Mol Biol 192:133–154
Lim M, Jackson TA, Anfirud PA (1995) Binding of CO to myoglobin from a heme pocket docking site to form nearly linear Fe-C-O. Science 269:962–966
Lim M, Jackson TA, Anfirud PA (1997) Ultrafast rotation and trapping of carbon monoxide dissociated from myoglobin. Nat Struct Biol 4:209–214
Natali F, Moretti L, Boffi F, Bianconi A, Della Longa S, Congiu Castellano A (1998) Light induced states in MbCO denatured with guanidine hydrochloride. Eur Biophys J 27:1–7
Ormos P, Brauenstein D, Frauenfelder H, Hong MK, Lin SL, Sauke TB, Young RD (1988) Orientation of carbon monoxide and structure-function relationship in carbonmonoxymyoglobin. Proc Natl Acad Sci USA 85:8492–8496
Ostermann A, Waschipky R, Parak F, Nienhaus U (2000) Ligand binding and conformational motions in myoglobin. Nature 404:205–208
Parak F, Hartmann H, Aumann KD, Reuscher H, Rennekamp G, Bartunik H, Steigemann W (1987) Low temperature X-ray investigation of structural distrbutions in myoglobin. Eur Biophys J 15:237–249
Pascarelli S, Neisius T, De Panfilis S (1999) Turbo-XAS: dispersive XAS using sequential acquisition. J Synchr Radiat 6:1044
Phillips SEV (1981) X-ray structure of deoxy-Mb (pH 8.5) at 1.4 Å resolution. Brookhaven Protein Data Bank
Pin S, Alpert B, Congiu Castellano A, Della Longa S, Bianconi A (1994) X-ray absorption spectroscopy of hemoglobin. Methods Enzymol 232:266–292
Powers L, Sessler JL, Woolery GL, Chance B (1984) CO bond angle changes in photolysis of MbCO. Biochemistry 2:5519–5523
Powers L, Chance B, Chance M, Campbell B, Khalid J, Kumar C, Naqui A, Reddy KS, Zhou Y (1987) Kinetic, structural and spectroscopic identification of geminates states of Mb: a ligand binding site of reaction pathway. Biochemistry 26:4785–4796
Takano T (1977) Structure of myoglobin refined at 2.0 Å resolution. J Mol Biol 110:569–584
Zhang K, Chance B, Reddy KS (1989) X-ray absorption near edge study of Mb and MbCO. Physica B 158:121–122